BBA - Molecular Cell Research 1868 (2021) 118971

Contents lists available at ScienceDirect

BBA - Molecular Cell Research

journal homepage: www.elsevier.com/locate/bbamcr

Human amylin aggregates release within exosomes as a protective mechanism in pancreatic β cells: Pancreatic β-hippocampal cell communication

J. Burillo [a,b,c], M. Fernández-Rhodes [a], M. Piquero [d], P. López-Alvarado [d], J.C. Menéndez [d], B. Jiménez [a,b], C. González-Blanco [a], P. Marqués [a], C. Guillén [a,b,c,*,1], M. Benito [a,b,c,1]

[a] Department of Biochemistry and molecular Biology, Complutense University, Madrid, Spain
[b] Centro de Investigación Biomédica en Red (CIBER) de Diabetes y Enfermedades Metabólicas Asociadas (CIBERDEM), Madrid, Spain
[c] MOIR2: Mechanisms of Insulin Resistance, General Direction of Universities and Investigation (CCMM), Spain
[d] Department of Organic Chemistry, Complutense University, Madrid, Spain

ARTICLE INFO

Keywords:
Exosomes
MVB
Amylin
Diabetes
Aggregates
Mitochondrial dynamics

ABSTRACT

Pancreatic β cells are essential in the maintenance of glucose homeostasis during the progression to type 2 Diabetes Mellitus (T2DM), generating compensatory hyperinsulinemia to counteract insulin resistance. It is well known, that throughout the process there is an increased mTORC1 signaling pathway, with an impairment in different quality control systems including ubiquitin-proteasome system and autophagy. In addition, under this situation, pancreatic β cells start to accumulate amylin protein (IAPP) in aggregates, and this accumulation contributes to the failure of autophagy, damaging different organelles such as plasma membrane, endoplasmic reticulum, mitochondria, and others. Here, we report that IAPP can be incorporated to multivesicular bodies (MVB) and secreted into exosomes, a mechanism responsible for the exportation of these toxic aggregates as vehicles of cell to cell communication. On this regard, we have demonstrated that the exosomes bearing toxic hIAPP released from pancreatic β cells are capable to induce hyperactivation of mTORC1 signaling, a failure in the autophagic cellular quality control, and favor pro-fission status of the mitochondrial dynamics in hippocampal cells. In summary, our results show that harmful accumulation of hIAPP in pancreatic β cells may be detoxified by the release of exosomes, which may be captured by endocytosis mechanism damaging neuronal hippocampal cells, which suggest an underlying molecular mechanism to the link between type 2 diabetes and neurodegenerative diseases.

1. Introduction

Exosomes are a type of small extracellular vesicles (EV) produced by different cell types under different conditions, including hepatocytes [1,2], adipocytes [3,4] and pancreatic β cells [5,6]. Very recently it has been proposed that exosomes could have a role in the communication among different organs under both basal and several stress situations [4,7,8]. These structures are produced by the endosomal pathway and specifically derived from the multivesicular bodies (MVB), by the formation of intralumenal vesicles (ILVs) that will origin exosomes [9]. The process is complicated and requires several steps which are regulated by the endosomal sorting complex required for transport (ESCRT 0-IV). Alternatively, there is another mechanism which is ESCRT-independent and needs the enzymatic activity of the neutral sphingomyelinase, an enzyme involved in ceramide synthesis and which levels have been related to exosome biogenesis [10].

Type 2 Diabetes Mellitus (T2DM) is a metabolic disease with two different stages. The first one is characterized by an increase in insulin levels, promoted by, at least in part, a hyperactivation of mTORC1 signaling in pancreatic β cells. This expansion gives rise to a boost in pancreatic β cell mass. In the second one, there is a reduction in insulin levels, mainly by a failure in the insulin secretion capacity and a reduction in pancreatic β cell survival [11,12]. Although the mechanisms that are involved in this failure in pancreatic β cells are not well

* Corresponding author at: Department of Biochemistry, Complutense University, Madrid, Spain.
E-mail address: cguillen@ucm.es (C. Guillén).
[1] Co-senior authors.

https://doi.org/10.1016/j.bbamcr.2021.118971
Received 12 July 2020; Received in revised form 19 January 2021; Accepted 24 January 2021
Available online 27 January 2021

understood, one possible explanation is the accumulation of amylin or islet amyloid polypeptide (IAPP), a hormone co-secreted with insulin, inside the cells. We have described that in INS1E overexpressing human amylin (hIAPP), there is an increase in mTORC1 signaling pathway, which negatively regulate the autophagic flux and turn outs in an accumulation of damaged mitochondria [13].

There are consistent evidence indicating a link between degradative pathways, and the secretory pathway [14–17]. It is well known that an alteration in autophagy function, as the main mechanism involved in the elimination of protein aggregates and defective or aged organelles, is associated with different pathologies, including cancer, T2DM and neurodegenerative diseases. Furthermore, MVB could be implicated in the secretion of misfolding proteins through exosomes. Indeed, exosome formation and secretion could be regulated by the autophagy-lysosome system. For instance, an autophagy stimulation with rapamycin or starvation inhibits exosome secretion in K652 erythroleukemic cell line, promoting the re-direction of MVB to the autophagic pathway [18]. In addition, it has been observed that in Parkinson disease (PD), where there is a defect in autophagy, exosome secretion bearing α-synuclein increases, favoring disease propagation [19–21].

In this paper, we propose that as a consequence of the autophagic blockade, because of the hyperactivation of mTORC1 observed in pancreatic β cells overexpressing hIAPP, there is an increased in the exosome secretion bearing hIAPP aggregates. This mechanism could serve as a detoxifying or protective mechanism for pancreatic β cells and could facilitate the accumulation of hIAPP in other organs, contributing to the connection of T2DM and its side effects such as diabetic nephropathy and neurodegenerative diseases.

2. Material and methods

2.1. Antibodies and reagents

The following primary antibodies were obtained from Cell Signaling Technology (Beverly, MA): anti-cleaved caspase 3 (#9661), anti-BiP (#3177), anti-LC3A/B (#4108), anti-phospho-p70S6K (Thr389) (#9205), anti-p70S6K (#9202), anti-phospho-ULK1 (Ser757) (#14202), anti-ULK1 (#6439), anti-PINK1 (#6946). Anti-hIAPP (ab103580), anti-insulin (ab7842) and anti-Parkin (ab77924) were obtained from Abcam (Cambridge, UK). Anti-CD63, anti-CD81 and anti-Hsp70 (EXOAB-KIT-1) were obtained from System-Biosciences (Palo Alto, CA). Anti-β-actin and anti-α-tubulin were obtained from Sigma-Aldrich (St. Louis, MO). Anti-hIAPP (IF) (NB600-713) was purchased to Novus Biologicals (Centennial, CO). Anti-OPA1 (#612607) was obtained from BD Biosciences (San Jose, CA). Anti-p62 (GP62-C-WBC) was obtained from ProGen (Heidelberg, Germany). Anti-Tsg101 (sc-7964) was obtained from Santa Cruz Biotechnology (Dallas, TE). Secondary antibodies HRP-conjugated used: anti-Rabbit (NA934) and anti-Mouse (NA931) were obtained from GE Lifesciences (Marlborough, MA). Anti-Guinea pig HRP-conjugated (90001) was purchased to ProGen (Heidelberg, Germany). Chloroquine (C6628), thapsigargin (T9033), GW4869 (D1692), dynasore (D7693) and phalloidin (P5282) were obtained from Sigma-Aldrich (St. Louis, MO). Carbonyl cyanide *m*-chlorophenylhydrazone or CCCP (038-16991) was purchased to Wako Chemicals (Neuss, Germany). Geneticin (G418) was obtained from Santa Cruz Biotechnology (Dallas, TE).

2.2. Cell lines

Rat insulinoma cell line INS1E were kindly provided by P. Maechler (Université de Genève, Geneva, Switzerland); INS1E overexpressing rat amylin (INS1E-rIAPP) and INS1E overexpressing human amylin (INS1E-hIAPP) were generously supplied by Anna Novials (IDIBAPS, Barcelona, Spain). INS1E cell lines were cultured in 10% FBS RPMI 1640 medium supplemented with 1 mM sodium pyruvate, 10 mM HEPES and 50 μM 2-mercaptoethanol. Mouse hippocampal cell line HT-22 was gently donated by Rafael Simó (Vall D'Hebron Research Institute, Barcelona, Spain) and cultured in 10% FBS DMEM High Glucose medium supplemented with 20 mM HEPES. SHSY-5Y neuroblastoma cell line was kindly provided by Ignacio Torres Aleman (Instituto Cajal, Madrid).

2.3. Exosome purification and labelling

To obtain purified exosomes, INS1E were cultured in 10% exosome-depleted FBS (Exo-FBS™) RPMI medium at 16,7 mM glucose concentration during 72 h. The different media were collected, centrifuged at 3000 ×*g* during 15 min to discard cellular debris, filtered by a 22 μm filter, mixed with Exo-Quick TC™ exosome isolation reagent and incubated at 4 °C with gentle shaking overnight. After that, the mixture was centrifuged at 1500 ×*g* for 30 min, obtaining an exosome-precipitate at the bottom of the tube. Isolated exosomes were resuspended in PBS 1× and added to cells, or resuspended and lysed RIPA buffer 1× to obtain exosome protein extract. To label exosomes, the isolating protocol was performed as previously described and then they were mixed, incubated and resuspended following Exo-Glow Membrane™ (EXOGM600A-1, SBI Bionova) or Exo-Glow Protein™ (EXOGP300A-1, SBI Bionova) protocol.

DLS

Exosomes resuspended in PBS 1× were diluted at a concentration range from 1 to 10 mg/ml to analyze them. 2 μl of the dilution was measured by Zetasizer Nano ZS (Malvern Instruments Ltd.) with a 633 nm laser. Data were obtained from 5 repeated measures at RT.

NTA

Exosome numbers and size distribution were measured from the rate of Brownian motion in a NanoSight LM10 system, which is equipped with fast video capture and particle-tracking software (NanoSight, Amesbury, UK). Briefly, 0.5 ml of diluted exosome fraction was loaded into the sample chamber of an LM10 unit (Nanosight, Amesbury, UK) and three 30-s videos were recorded of each sample. Data were analyzed with NTA 2.1 software (Nanosight). Samples were analyzed using manual shutter and gain adjustments, which resulted in shutter speeds of 15 or 30 ms, with camera gains between 280 and 560. The detection threshold was kept above 4; blur: auto; minimum expected particle size: 50 nm. Samples were diluted before analysis to concentrations between 2 × 108 and 20 × 108 particles/ml.

2.4. Western blotting

After the different treatments, cells were washed twice with PBS 1× and lysed for protein extraction according to standard procedures. Protein concentration determination was achieved by the Bradford dye method, using de Bio-Rad® (Hercules, CA) reagent and BSA as standard. Equal amounts of protein (15–20 μg) were submitted to electrophoresis and after SDS-PAGE gels were transferred to Immobilon P PVDF membranes (Merck Millipore, Burlington, MA). Then, membranes were blocked with 5% BSA and incubated overnight with primary antibodies at 4 °C. The corresponding bands were visualized using the ECL Western blotting protocol (GE Healthcare, Little Chalfont, UK).

2.5. Immunofluorescence

Cells were grown on glass coverslips and fixed using paraformaldehyde 4% solution during 20 min, permeabilized in PBS with 0,5% Triton X-100 for 15 min, and then blocked with blockage solution (3% BSA, 0,1% Tween 20 in PBS) for 1 h. Cells were incubated overnight at 4 °C with primary antibodies (1:50 in blocking solution). After the incubation, coverslips were incubated with the corresponding secondary antibodies at a dilution of 1:100 for 1 h 30 min. For MG5 imaging, the organic compound was diluted in DMSO to 10 μM, and cells were incubated with the solution for 20 min before DAPI staining. For co-localization analysis, the images were processed with Coloc2 (http://fiji.sc/Fiji). We chose different region of interest (ROI) (at least 3 ROI of 3 different images) and the threshold was obtained automatically using Coste's automatic threshold, determining the Pearson's

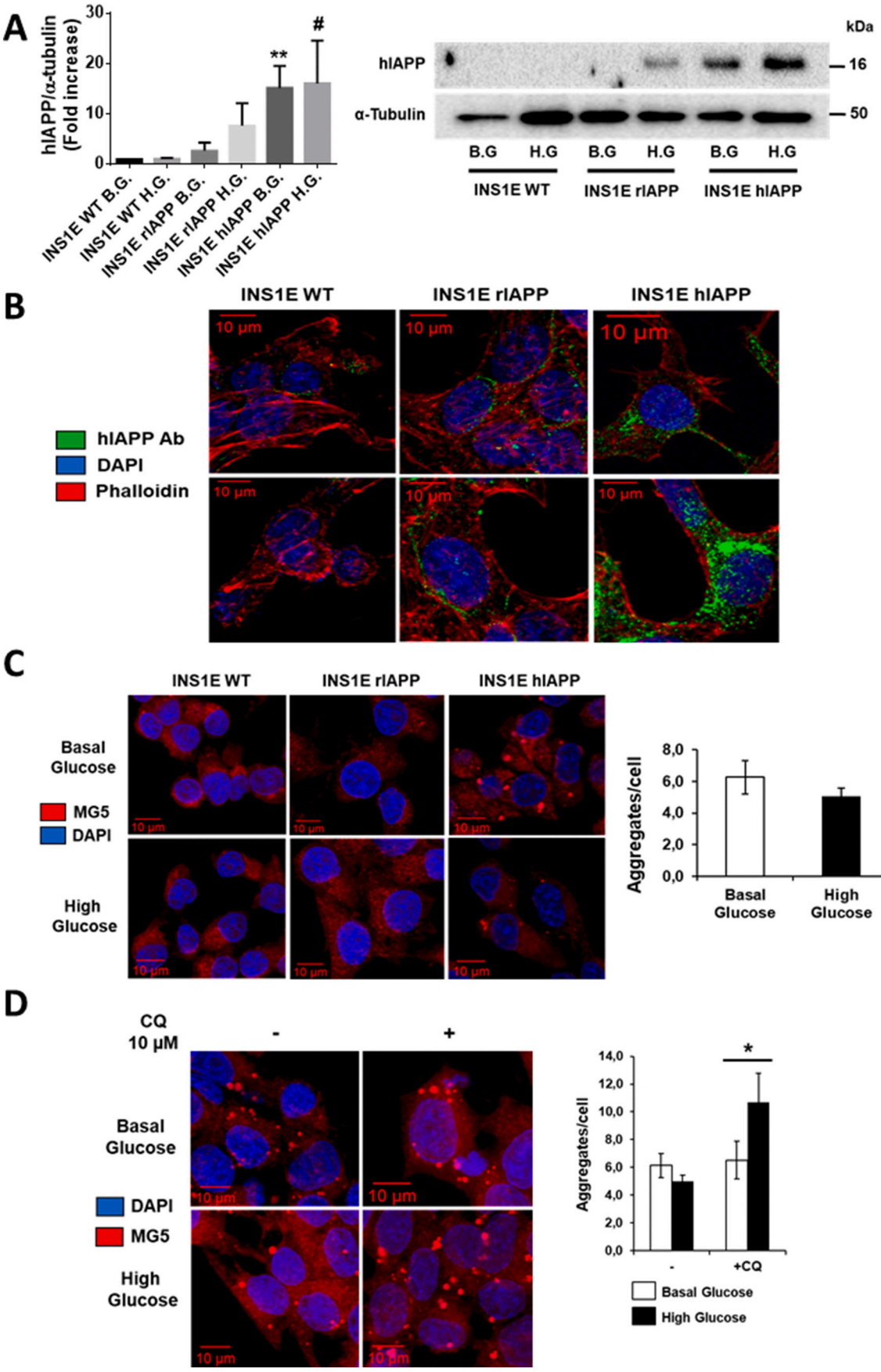

(caption on next page)

Fig. 1. INS1E hIAPP cells produce amylin aggregates in the cytosol that diminish under high glucose conditions. (A) Immunoblot analysis of amylin, using β actin as loading control, in the cell extracts of the 3 different pancreatic β cell lines exposed to either low or high glucose levels (n = 3). The plot indicates the quantification data of hIAPP/β-actin ratio under the different conditions. (B) Immunofluorescence staining using antibodies against amylin and phalloidin in the different pancreatic β cells under either low or high glucose levels. DAPI staining was used to detect nuclei (n = 3). (C) Immunofluorescence staining using MG5 compound, which detects amylin aggregates analyses in the different pancreatic β cells. The plot indicates the mean of aggregates/cell comparing basal and high glucose conditions in INS1E-hIAPP cells. Data represent the mean ± standard error of the mean (SEM) (n = 5). (D) Immunofluorescence analysis of INS1E-hIAPP under either low or high glucose levels in the presence or the absence of chloroquine (CQ) for 8 h. Data represent the mean ± standard error of the mean (SEM). Differences were determined by unpaired Student *t*-test analysis comparing black bars (mean of the number of aggregates per cell under high glucose levels pre-treated or not with CQ). *, $p < 0,05$ (n = 5).

correlation coefficient (PCC). For analyzing the number of aggregates per cell, we used at least 70 cells per condition obtained from 3 different experiments. After determining a threshold, we analyzed the number of elements, using the plug-in "count particles". This value was divided for the number of nuclei in the slide, obtaining the mean number of aggregates per cell. For the experiments of inhibition of endocytosis, we pre-treated HT-22 cells with dynasore at 80 μM for 90 min. Afterwards, we stimulated cells with the exosomes obtained from INS1E-hIAPP for 4 h. Then, cells were fixed and permeabilized as explained before and then, cells were treated with DAPI staining.

2.6. Violet crystal staining

SHSY-5Y and HT-22 cell lines were seeded in 12-well plates at a density of 5000 cells/cm^2 in 10% FBS DMEM medium. After 24 h, cells were treated with thapsigargin 1 μM, INS1E WT and r/hIAPP fresh media, and 48 h INS1E rIAPP and hIAPP supernatant for 24 h. Then, cells were washed twice with cold PBS and then stained with 0,2% violet crystal (w/v) in 2% ethanol (v/v) for 10 min. Plates were rinsed with ddH2O, dried, and after addition of 1% sodium dodecyl sulfate (w/v), absorbance at 560 nm was determined for each experimental point.

2.7. Electron microscopy

After exosome isolation following the protocol previously described, exosomes in PBS were fixed in 4% paraformaldehyde (Electron Microscopy Sciences, 15710) and 2,5% glutaraldehyde grade I (Sigma, G8882) in 0,1 M sodium phosphate buffer (pH 7,3) for 3 h. Samples were postfixed in 1% OsO4 (Electron Microscopy Sciences, 19172), 1,5% K4 [Fe(CN)6] for 1 h, dehydrated with acetone, and embedded in Epon812 (TAAB, T004). Thin sections (60–70 nm) were obtained with an Ultracut E (Leica) ultramicrotome, stained with lead citrate, and examined under a JEM-1010 transmission electron (JEOL).

2.8. Statistical analysis

Statistically significant differences between mean values were determined using the unpaired Student's *t*-test in the Graphpad statistical analysis software package. Differences were considered statistically significant at $p < 0,05$ (*/# $p < 0,05$; **/## $p < 0,01$; *** $p < 0,005$; n. s. indicates no statistical significance).

3. Results

3.1. INS1E hIAPP cells accumulate amylin aggregates in the cytosol under low glucose and clear out under high glucose conditions

Firstly, we detected amylin protein in cellular extracts obtained from the different cell lines using an antibody, which is capable to recognize this protein in several species. Using this strategy, we observed a higher accumulation of amylin, especially in INS1E overexpressing hIAPP under basal glucose levels (INS1E-hIAPP). When we exposed the cells to high glucose levels, we observed a further increase in amylin production, more evident in INS1E hIAPP (Fig. 1A). Interestingly, the predicted molecular size using this antibody is 10 kDa, which corresponds to pre-pro-amylin protein. In contrast, in our hands, we observed a band at around 16 kDa. Using the previous antibody in immunofluorescence, we corroborated the increased accumulation of amylin under high glucose levels (Fig. 1B). We used phalloidin antibody just to delineate cell periphery and determine cellular limits. In collaboration with the Organic Chemistry department of our faculty, we used an organic fluorescent compound (this structural analogous here is named MG5) that is capable to detect β-sheet aggregates as it was previously described [22]. We observed that only in INS1E-hIAPP there was an accumulation of these aggregated structures in dots localized inside the cells in the basal state. Interestingly, there was a tendency to the reduction in the number of aggregates in response to high glucose levels (Fig. 1C). To analyze the involvement of autophagy in the clearance of these aggregates, we blocked the autophagic flux by using chloroquine (CQ). When we used CQ, we observed a higher accumulation of MG5, especially in high glucose concentration, indicating a role of autophagy in the clearance of these aggregates under these conditions (Fig. 1D). We did not detect the expected increase of aggregates in CQ-treated cells under basal glucose conditions because of the low dose of chloroquine utilized (10 μM) in order to not interfere with cell viability. However, we cannot rule out other possible mechanisms apart from autophagy in the reduction of amylin aggregates after exposure to high glucose levels. Our group published that INS1E-hIAPP presents a mTORC1 hyperactivation, inducing a blockade in both the autophagic as well as in the mitophagic flux [13]. As it was mentioned in the introduction, degradative pathways are interconnected with the secretory pathway. For testing this possible link, we analyzed whether the alteration in autophagic flux observed in INS1E-hIAPP has any consequence in its secretion profile, inducing possible disturbances in other cell lines. For that purpose, we collected the whole secretome (48 h supernatant) from the different INS1E cell lines and added to two different neuron-like cells such as a neuroblastoma cell line (SH-SY5Y) and a mouse hippocampal cell line (HT-22). We observed that the supernatant obtained from INS1E-hIAPP was capable of decreased cell survival in both neuron-like cell lines (Supplemental Figs. 1A, B and 2). Furthermore, INS1E-hIAPP supernatant induced a higher level of LC3B lipidation compared with the supernatant obtained from the other cell types, which potentially suggests an induction of autophagy (Supplemental Fig. 1C). Collectively, these results indicate the existence of a secreted factor, produced by INS1E-hIAPP, which could mediate the changes observed in both SHSY5Y and HT-22 cell lines.

3.2. hIAPP aggregates are processed in the MVB in an ESCRT-dependent manner

For testing other possible strategies in the elimination of amylin aggregates (MG5), we explored whether the ESCRT system is involved in the processing of these structures. We observed an intense co-localization signal between Tsg101 protein, an ESCRT-I complex protein involved in the production of ILVs into the MVB [23], with MG5 under low glucose conditions (Fig. 2A and B). Very interestingly, after increasing glucose levels, there was a reduction in the co-localization signal (Fig. 2A and B). These results indicate that amylin aggregates are processed by the endosomal sorting machinery. In contrast, soluble hIAPP did not co-localize with MG5 neither under low nor high glucose concentrations, suggesting a specific interaction of the ESCRT machinery with the aggregates and not with soluble hIAPP (Fig. 2C, D). In

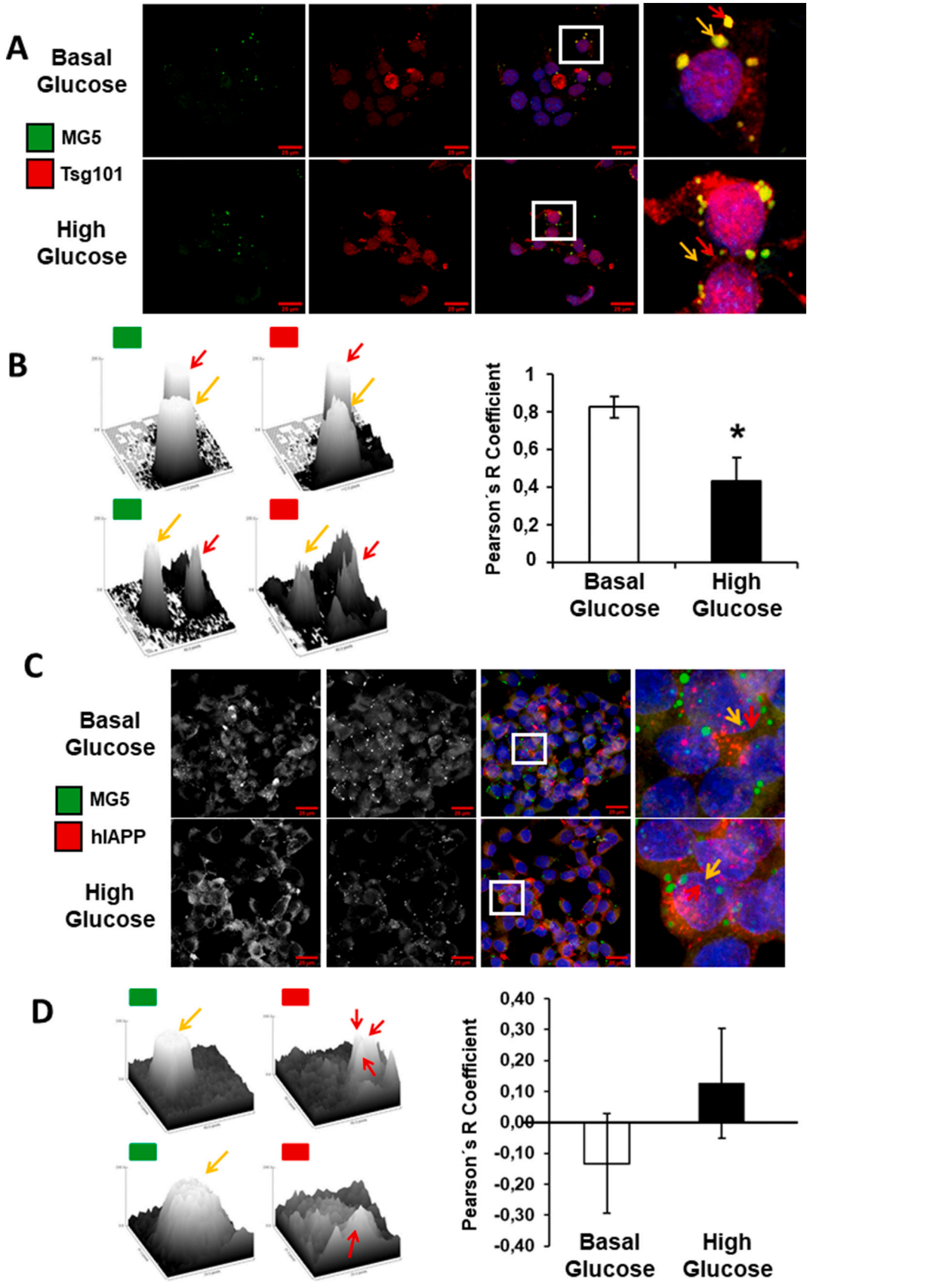

(caption on next page)

Fig. 2. hIAPP aggregates are processed in the MVB in an ESCRT-dependent manner. (A) Immunofluorescence of INS1E-hIAPP pancreatic β cells under basal and high glucose conditions using MG5 compound (which detects amylin aggregates) and anti-Tsg101. The corresponding surface plots of two regions of interest (ROI) are indicated by the arrows (red and orange) and are shown beside the images (n = 4). (B) Plot indicating Pearson's coefficient corresponding to the thresholded images of the colocalization analysis of amylin aggregates, using MG5 compound, and Tsg101 antibody, under low or high glucose conditions. Differences were determined by unpaired Student t-test analysis (*p < 0,05). Data represent the mean ± standard error of the mean (SEM) (C) Immunofluorescence of INS1E-hIAPP pancreatic β cells under basal and high glucose conditions using anti-amylin and MG5 compound. The corresponding surface plots, indicated by the arrows (red and orange), are shown beside the images (n = 4). (D) Pearson's coefficient corresponding to the thresholded images of the colocalization analysis of amylin aggregates, using MG5 compound, and amylin antibody.

contrast, hIAPP did co-localize with insulin under basal levels, being more evident, after high glucose concentration (Supplemental Fig. 3). Taken together, these results suggest that hIAPP aggregates are processed into the ESCRT machinery by the intense signal of Tsg101 and MG5. Furthermore, the decrease signal observed after increasing glucose concentrations, point to higher processing under these conditions.

3.3. Human amylin is released from pancreatic β cells and vehicled by exosomes

It is well known that amylin is secreted by pancreatic β cells in a soluble manner by the canonical secretory pathway [24]. However, it is also true that INS1E-hIAPP has a defect in both insulin and amylin secretion after the exposure to high glucose levels [25]. After the observation of the co-localization of MG5 aggregates with the ESCRT machinery, we decided to analyze whether amylin aggregates could be trafficked through exosomes, as a non-canonical pathway of elimination. We purified, lysed and characterized exosomes obtained from the different cell lines INS1E WT, INS1E rIAPP and INS1E hIAPP. First, we confirmed a correct purification of exosomes by the detection of CD63 and CD81, two exosomal markers which belongs to the tetraspanins family, and another exosomal marker such as Hsp70. To assess the specificity in the isolation, we checked the absence of other proteins belonging to Golgi apparatus, such as GM130 or golgin. As it can be observed, there was no signal of GM130 in the exosome fraction (Fig. 3A). When we analyzed amylin levels in the protein extract from exosomes, we detected an increased amylin content in exosomes from INS1E-hIAPP, with a higher molecular weight than expected for pre-pro-IAPP using this antibody, indicating the capacity of secreting amylin aggregates inside exosomes by this cell line under high glucose levels (Fig. 3A). For further characterization, we challenged the exosome fraction to dynamic light scattering (DLS) analysis. Using this technique, we observed a medium size of 24 nm in INS1E-WT, 18 nm in INS1E-rIAPP and a range from 14 to 37 nm in INS1E-hIAPP (Fig. 3B). In fact, there were no significant differences among the exosomes as is indicated in the plot of the exosome average size. These observations were corroborated using the nanoparticle tracking analysis (NTA) (Supplemental Fig. 4). The electron microscopy images indicated the correct purification of exosomes in intact round vesicles of around 30 nm in size (Fig. 3C).

3.4. The blockade of MVB secretion induces an accumulation of amylin aggregates inside INS1E-hIAPP cells and an increase in cell apoptosis

Using GW4869, an exosome secretion inhibitor by blocking the neutral sphingomyelinase (n-SMase) activity, we observed an accumulation of amylin protein levels either under basal glucose or under high glucose concentration (Fig. 4A and B). However, there was a reduction in amylin protein levels with the increasing time of exposure to the inhibitor (Fig. 4A and B). These data potentially suggest that amylin, which is not secreted properly by these cells, could be recruited to exosomes and expulsed by an alternative pathway, which is not inhibited by GW4869, for reducing the potential toxic forms of amylin. As it was previously mentioned, the molecular weight of amylin was higher than the expected for pre-pro-amylin. Concomitantly, when we used this inhibitor, there was a dramatic increase (about 10-fold) in cleaved caspase-3 levels, suggesting that exosome secretion has a protective role in these cells under normal conditions as well as under high glucose levels. When we used CQ, for autophagic flux inhibition, there was a slight increase in apoptosis, and there was no further increased when it was used in combination with GW4869 (Fig. 4C and D). Then, for analyzing the efficacy of GW4869 in exosome secretion inhibition, we determined the exosome marker CD63, inside the cells or in the supernatant in the presence of increasing concentrations of GW4869 under either low or high glucose concentrations. Using this strategy, we observed a tendency either in the accumulation in CD63 protein level inside the cell as well as in the decreased in the supernatant after the addition of the inhibitor in a dose-dependent manner, although the changes were not statistically significant (red squares) (Fig. 4E and F). These results suggest that firstly, INS1E-hIAPP presents an important production of these structures in the basal state and secondly, there is a partial effect of the inhibitor in blocking exosome secretion. Something similar was also observed under high glucose concentration (blue squares) (Fig. 4E and F). As expected, when we treated the cells with the GW4869 at basal glucose, there was an increased in MG5 aggregates inside the cell (Fig. 4G, upper panels). Paradoxically, under high glucose in the presence of the inhibitor, there was a decrease in the number of aggregates compared with basal glucose conditions (Fig. 4G, lower panel). Then, this paradoxical effect of the inhibitor in MG5 aggregates point to the co-existence of an alternative secretory mechanism of aggregates in an n-SMase-independent manner. Then, these data highlight the ESCRT-dependent pathway as another alternative in exosome secretion. Altogether, these observations suggest that exosome secretion of amylin aggregates represents a protective mechanism in INS1E-hIAPP either under basal conditions or under high glucose conditions.

3.5. Exosomes released by pancreatic β cells bearing human amylin are internalized by endocytosis in HT-22 neuronal hippocampal cells

Then, we purified the exosomes from INS1E-hIAPP pancreatic β cells and, after fluorescence labelling, we exposed mouse hippocampal neuron-like cell line (HT-22) to the exosomes. We demonstrated that indeed the exosomes were captured by HT-22 cells in a time-dependent manner (Fig. 5A). In addition, we also analyzed the possible involvement of endocytosis in the uptake of exosomes from HT-22 cells. Then, we pre-treated the cells with the inhibitor dynasore, which blocks the essential GTPase activity of dynamins in the generation of the endocytic particle [42]. After the treatment with dynasore and exposure to the labelled exosomes, we did not detect any fluorescent signal in the interior of HT-22 cells, suggesting a key role of endocytosis in the capture by the recipient cells, HT-22 cells (Fig. 5B).

3.6. Exosomes obtained from INS1E-hIAPP cells alter the autophagic flux and favor pro-fission status of the mitochondrial dynamics in HT-22 cells

In order to analyze the consequences of exosome exposure in neuron-like cells, we treated HT-22 cells with the exosomes obtained from INS1E-hIAPP. We observed a strong induction of mTORC1 signaling pathway with a significant increase in phospho-ULK1 Ser 757 and phospho-p70 Thr 389 signals (Fig. 6A). Furthermore, we observed a tendency in the accumulation of both p62 and LC3B protein levels, suggesting an initial impairment in autophagic flux, although the changes were not statistically significant (Fig. 6B). This tendency in the accumulation of PINK1 and PARKIN protein levels were also observed,

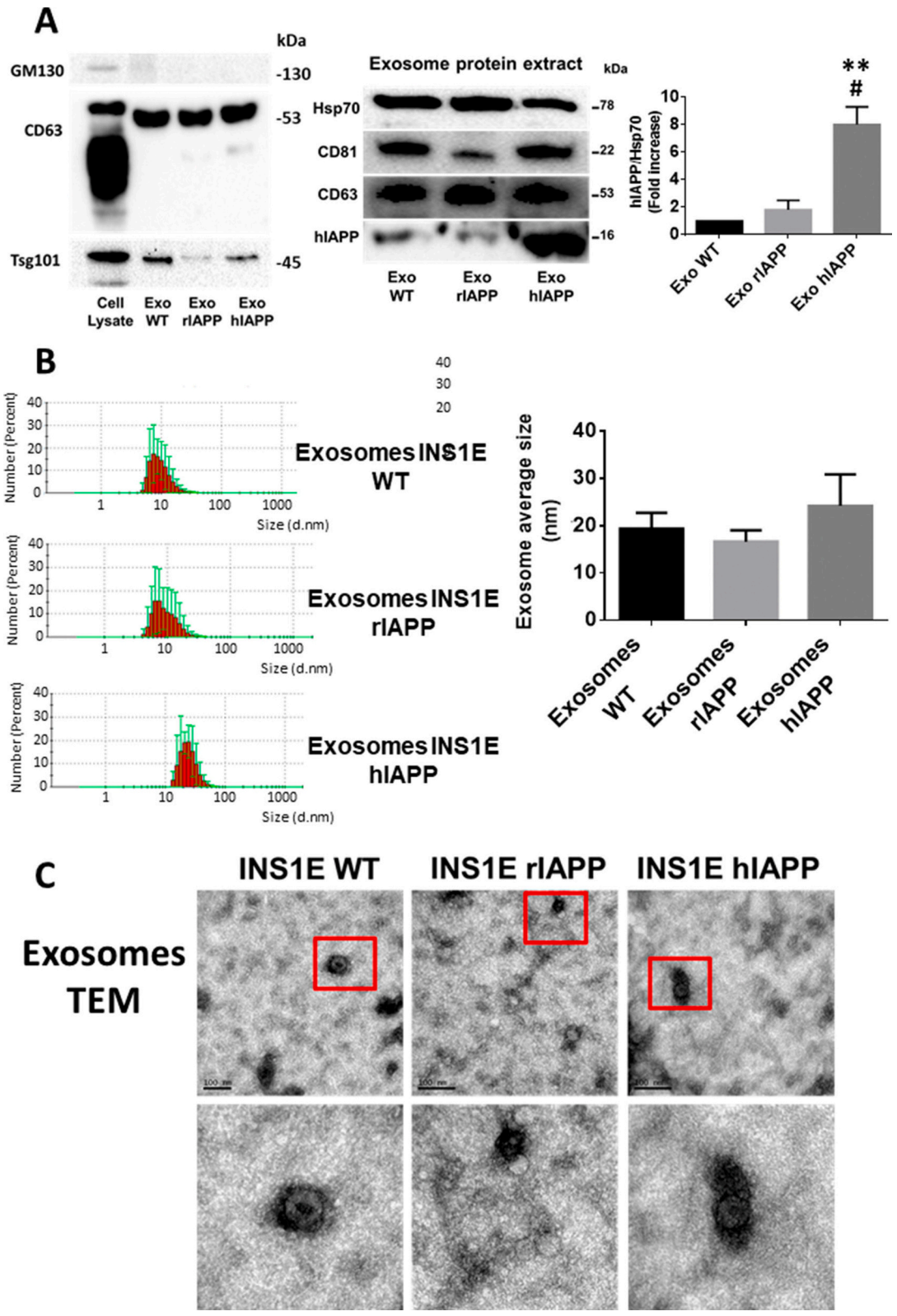

Fig. 3. Human amylin is exported from pancreatic β cells using exosomes. (A) Immunoblot analysis of the exosomal protein extract obtained from the supernatant of the different pancreatic β cells (INS1E WT, INS1E-rIAPP and INS1E-hIAPP) grown under high glucose conditions. Fold increase of amylin (IAPP) protein levels relative to Hsp70 protein levels comparing the different pancreatic β cells. **$p < 0,01$ comparing exosomes WT versus exosomes obtained from INS1E-hAPP and $^{\#}p < 0,05$ comparing exosomes INS1E rIAPP versus exosomes from INS1E-hIAPP. Data represent the mean ± standard deviation (SD) ($n = 3$). (B) Dynamic light scattering analysis of the exosomes purified from the different pancreatic β cells ($n = 5$). (C) Electron microscopy images from the exosomes obtained from the different pancreatic β cells (upper panels). An amplification view of the exosomes is shown (lower panels). Scale bar, 100 nm in the inset ($n = 3$).

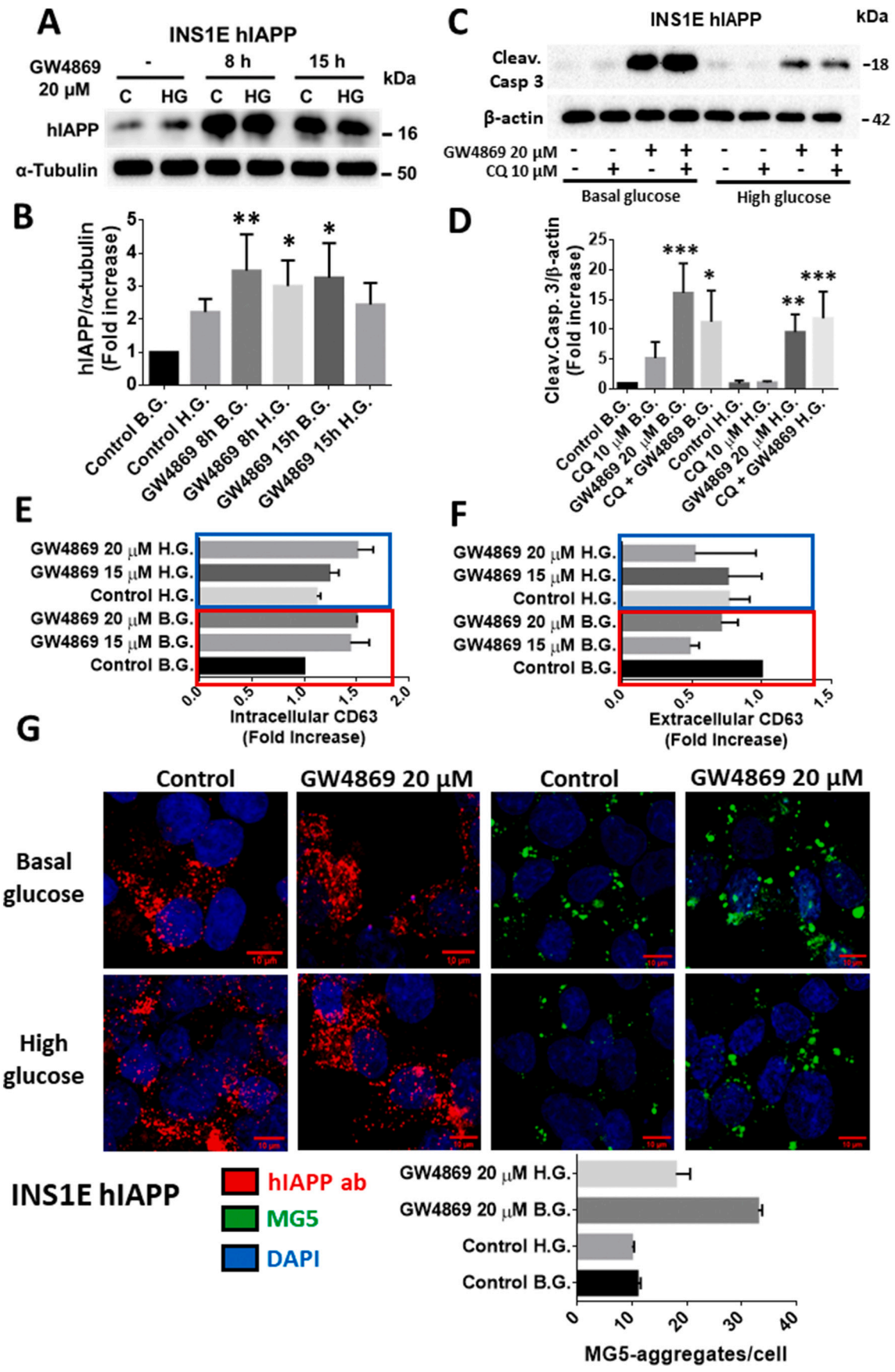

(caption on next page)

Fig. 4. The blockade of MVB secretion induces an accumulation of amylin aggregates inside INS1E-hIAPP cells and an increase in cell apoptosis. (A) INS1E-hIAPP pancreatic β cells were pre-treated with the exosome inhibitor GW4869 at different time points (8 and 15 h) under either low glucose or high glucose conditions and the hIAPP and α-tubulin proteins were analyzed by western blotting (n = 4). (B) Plot representing the hIAPP/α-tubulin ratio under the different conditions studied. Differences were determined by unpaired Student t-test analysis comparing each bar with the respective control under basal glucose (n = 4). *p < 0,05; **p < 0,01. (C) INS1E-hIAPP pancreatic β cells were pre-treated with the exosome inhibitor GW4869 in the presence or in the absence of CQ under either basal or high glucose concentrations. Then, cleaved caspase-3 protein levels and β-actin were analyzed by western blotting (n = 6). (D) Plot representing the fold-increase in cleaved caspase-3/β-actin ratio under the different conditions studied. Differences were determined by unpaired Student t-test analysis comparing each bar with the respective control under basal glucose. *, p < 0,05; **p < 0,01, ***p < 0,005. Data represent the mean ± standard deviation (SD). (E) intracellular (n = 3) and (F) extracellular (n = 3) CD63 protein levels in response to different doses of GW4869 under either low or high glucose levels. (G) Immunofluorescence staining in INS1E-hIAPP cells using both hIAPP antibody and DAPI staining or MG5 and DAPI under basal or high glucose concentrations in the presence or the absence of GW4869.

suggesting an initial, and not statistically significant, impairment in mitophagy (Fig. 6C). Very interestingly, we also observed a tendency towards a more fissioned state of mitochondria by the appearance of an increase, although not statistically significant, in OPA-1 short isoform and P-DRP1 Ser616, which are involved in mitochondrial fission, after the treatment with these exosomes (Fig. 6D). Importantly, a significant increase in apoptosis was also observed after the exposure to hIAPP aggregates-bearing exosomes, suggesting a deleterious effect in HT-22 hippocampal neuron-like cell line (Fig. 6E).

4. Discussion

T2DM is a complex metabolic disease that it is characterized by insulin resistance, inducing a compensatory mechanism in pancreatic β cells to counteract this effect. Our group and many others have contributed to a better understanding of the underlying molecular components that could have a role in this response. It is well established that mTORC1 hyperactivation is essential for the first phase of pancreatic β cell compensation [12,26–28]. However, chronic hyperactivation of mTORC1 is deleterious and drives pancreatic β cells to a failure, inducing the appearance of T2DM [12,26]. Very recently, hIAPP accumulation has also been involved in the activation of mTORC1 in pancreatic β cells [13]. Chronic mTORC1 activity generates a disruption of autophagy, which represents a protective mechanism, facilitating hIAPP aggregation as well as an alteration in the degradative capacity of these cells [13,29,30]. The present study shows that hIAPP aggregation inside pancreatic β cells induces a detoxifying mechanism through the formation of exosomes bearing hIAPP, through both ESCRT-dependent and ESCRT-independent pathways. In all the experiments using amylin antibody by western blot analysis, we always observed a higher molecular weight band that the expected. Nonetheless, our simplest interpretation is that this band corresponds to the aggregation capacity of amylin generating a band of 16 kDa, which fits with the production of a tetramer association of amylin. Although our results were obtained in vitro, it is a challenge to corroborate the implication of this pathway in vivo. This mechanism could facilitate the access of aggregated hIAPP protein to extra-pancreatic regions, including the brain, being a plausible explanation for the higher incidence of cognitive decline and Alzheimer's disease among type 2 diabetics [31,32]. Then, if this mechanism could operate in vivo, a new avenue of research connecting diabetes and Alzheimer's disease would be opened, which is the production of exosomes bearing aggregated amylin. In this regard, hIAPP transgenic mice in β islets fed on high-fat diet (HFD) revealed hIAPP into the hippocampus of those mice, contributing to brain aging and the appearance of mental deterioration [33]. Hereof, hIAPP is directly involved in production of the toxic forms of Aβ and its deposition, linking T2DM and AD [34]. In addition, different models of T2DM showed a compromised hippocampal neurogenesis [35]. Collectively, these data suggest that under pre-diabetic conditions, amylin could have potentially deleterious effects on this region of the brain, facilitating Aβ accumulation observed in those diabetic patients that develop Alzheimer's disease.

Our data indicate the existence of a constitutive production of exosomes bearing hIAPP in INS1E-hIAPP. However, it seems that under high glucose levels, amylin is more efficiently conveyed into exosomes, since we observed a reduction in the number of aggregates inside the cells and a decreased in co-localization signal between aggregates and the ESCRT machinery. These data indicate that amylin aggregates, although we cannot rule out the possibility of amylin as well, is packaged into exosomes and secreted to the extracellular milieu. If this process constitutes a protective mechanism of the cell to cope with the accumulation of amylin aggregates, the downregulation of this mechanism would alter cell viability, because of a great accumulation of these structures inside the cell. In this regard, when we treated the cells with GW4869, there was an important induction of cleaved caspase-3 levels (about 10-fold induction). Accordingly, using this inhibitor we observed an increase in MG5 positive aggregates, but the tendency of reduction in the number of aggregates under high glucose previously observed is maintained. Probably, the effect of GW4869 is partial and the decrease of aggregates could correspond to an ESCRT-dependent exosome formation mechanism, as our data suggests. In fact, we observed an intense co-localization signal between Tsg101, one of the ESCRT components, with amylin aggregates. This process of exosome secretion seems to be a detoxifying mechanism as it has been proposed in other pathologies such as Parkinson's disease [36,37], Alzheimer's disease [19,38] and many other diseases. Very interestingly, in the case of TDP-43, the toxicity is higher when the recipient cells take-up the aggregated protein from the exosomes than the free form protein [36]. This exosome-mediated mechanism could have higher detrimental effects on the recipient cells than those observed with the free protein, which it is known that is able to decrease cell viability in other pathologies such as neurodegenerative diseases.

For analyzing in vitro this interaction between pancreatic β cells and neuron-like cells, we explored the role of the exosomes obtained from INS1E-hIAPP in the hippocampal cells, HT22. Before that, we corroborated that HT-22 were indeed capable to incorporate exosomes from INS1E-hIAPP. In fact, our data indicate that endocytic machinery is essential for the introduction of these exosomes in the interior of the recipient cells. The experiments indicate that a pre-treatment with dynasore, could avoid the inclusion of exosomes-bearing hIAPP aggregates into HT22 cells. Beside endocytosis, several additional mechanisms may be involved such as phagocytosis, micropinocytosis and fusion with the plasma membrane [39], However, endocytosis is one of the main regulators, since dynasore pre-treatment, abolished the capture of exosomes by HT22 cells. In HT22 cells, upon exposure to these exosomes, we observed several deleterious alterations that we had previously found in pancreatic β cells overexpressing human amylin (INS1E-hIAPP) [13]. The exposure of these exosomes induced a statistically significant mTORC1 activation, and the accumulation of p62 and LC3B protein levels indicate some failure in autophagy process. In addition, there was a tendency to unbalance the mitochondrial dynamics by an increase in phospho-DRP1 and Opa-1 S/L ratio pro-fission proteins versus MFN-1 and MFN-2, fusion proteins. Furthermore, there was an accumulation, although not statistically significant, in PINK1 and PARKIN proteins. These data suggest that the exposure of HT-22 to the INS1E-hIAPP exosomes somehow alters mitochondrial membrane potential, which is responsible for the accumulation of PINK1 and PARKIN, involved in mitophagy. These data probably indicate an accumulation of

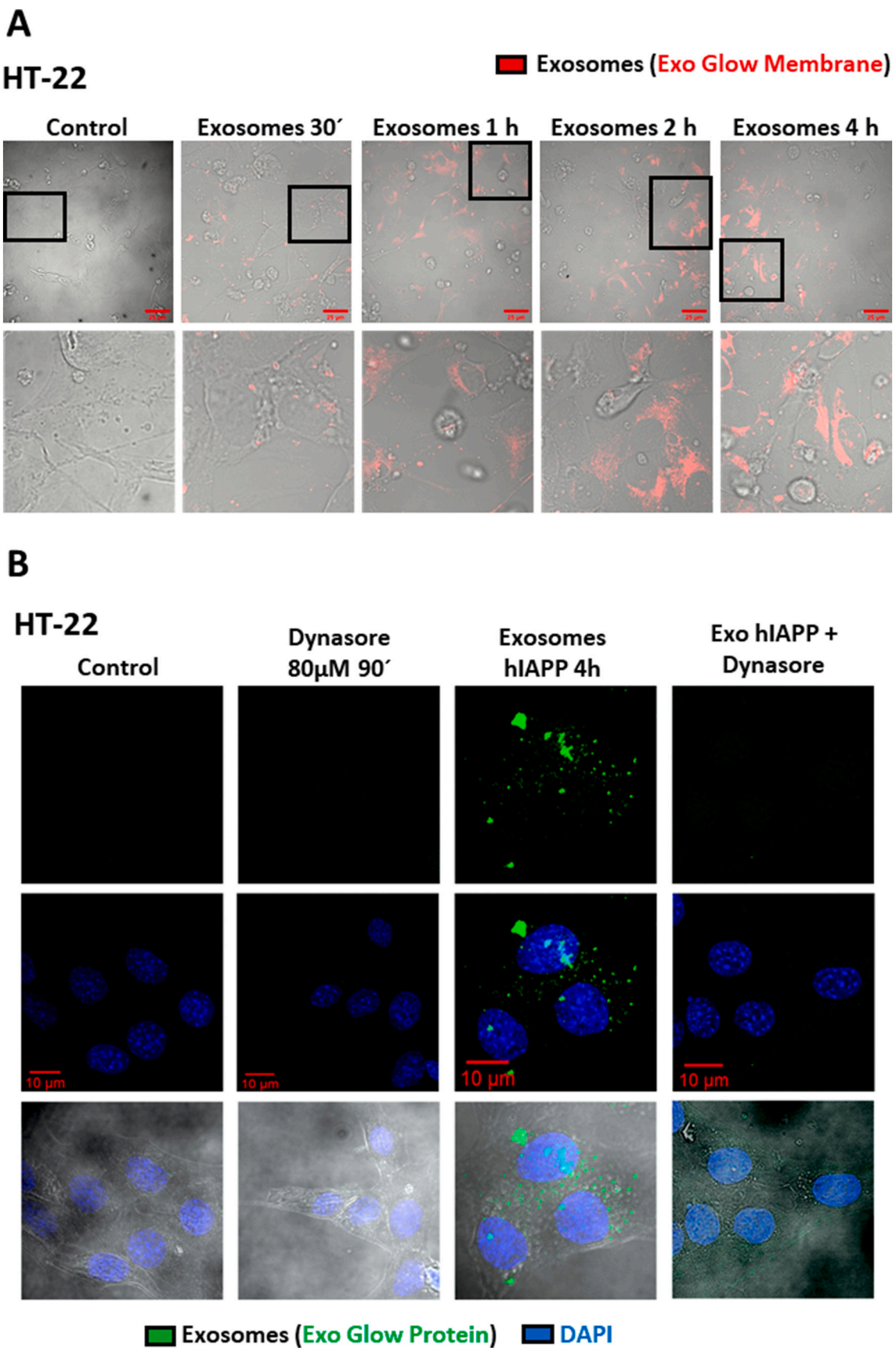

Fig. 5. hIAPP aggregates-bearing exosomes are internalized by endocytosis into HT-22 cells. (A) HT-22 hippocampal neuron-like cells were treated for 4 h with the exosomes purified and labelled with the Exo-Glow Membrane™. Different photographs were taken at different time points (30 min–4 h) (n = 3). (B) Exosomes-bearing hIAPP aggregates were labelled with Exo-Glow protein. HT-22 was pre-treated or not with dynasore at 80 µM for 90 min and the exosomes were added for 4 h. After that, cells were fixed, permeabilized and stained with DAPI.

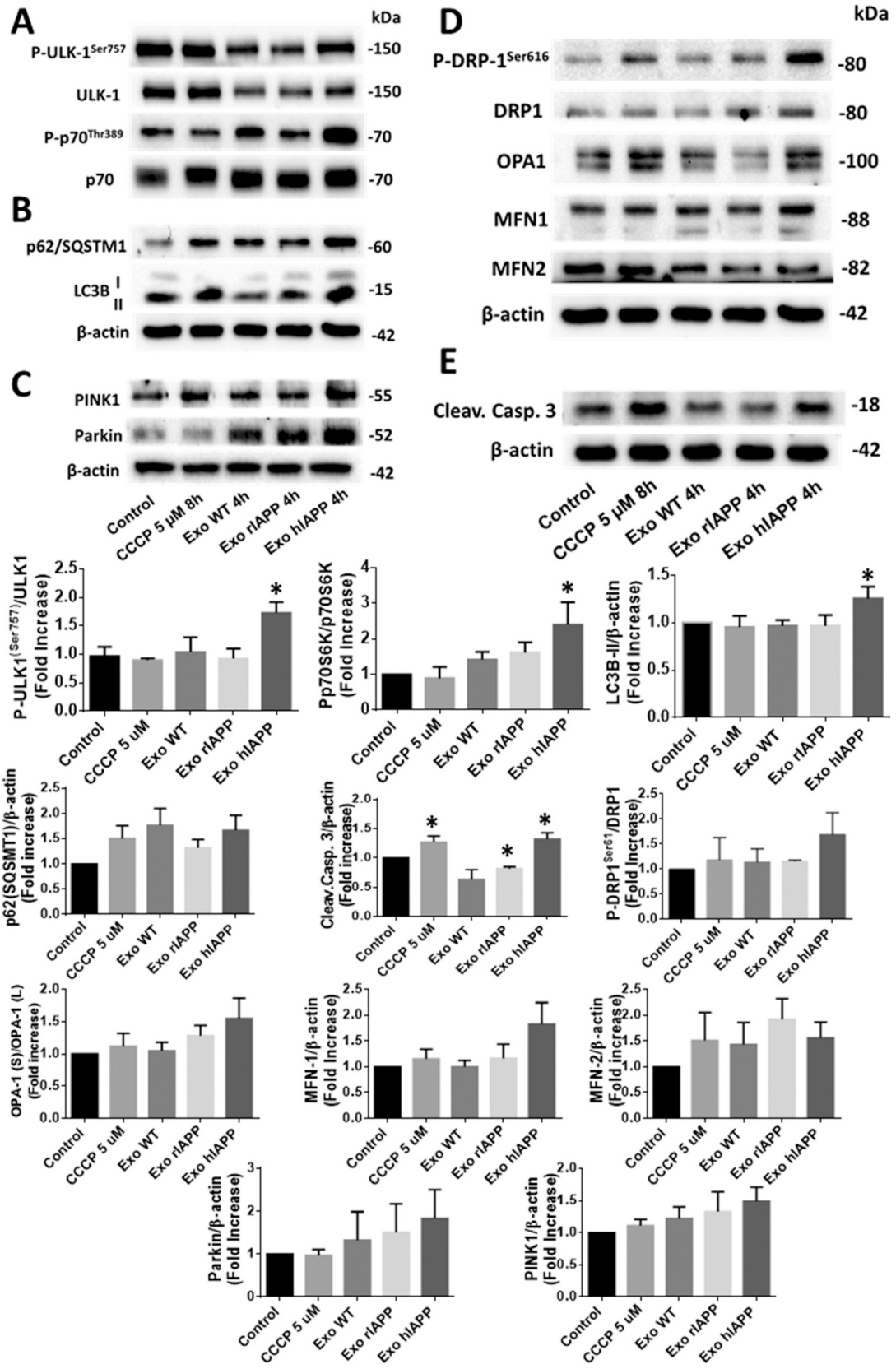

Fig. 6. Exosomes released from INS1E-hIAPP cells alters autophagic flux and mitochondrial dynamics in HT-22 hippocampal cells. (A) HT-22 cells were treated with the exosomes obtained from INS1E-hIAPP cells for 4 h. Then, proteins were extracted from cell culture, and afterwards, the proteins were studied by immunoblot analysis. The corresponding densitometric analysis corresponding to (left part of the panel); mTORC1 signaling pathway: phospho-ULK1 Ser 757, ULK1, phospho-p70 Thr 389, p70; autophagy: p62/SQSTM1, LC3B I and II and apoptosis: cleaved caspase-3 protein levels. (B) HT-22 cells were treated as in (A) and the blots and its corresponding densitometric analysis for studying mitophagy; phospho-DRP1 Ser 616, DRP1 PINK1 and PARKIN protein levels and mitochondrial dynamics: OPA-1, MFN-1, MFN-2, were analyzed. Densitometric analysis was determined in all the proteins (n = 5). Data represent the mean ± standard deviation (SD).

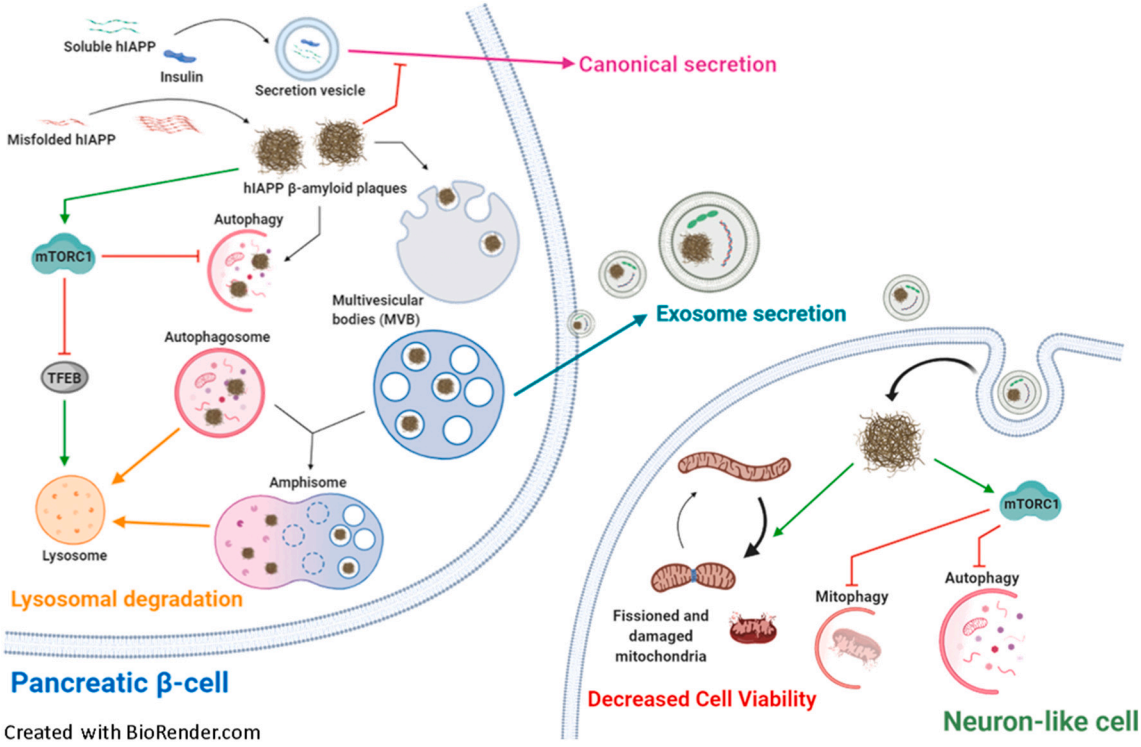

Fig. 7. Scheme depicting the changes observed in pancreatic β cells overexpressing hIAPP on mTORC1 signaling pathway, exosome production and blockade in autophagic flux. In addition, in this scheme, it is focused the effect of exosome-bearing amylin aggregates on neuron-like cells.

fissioned and labelled mitochondria, which are not properly degraded by autophagy. More importantly, hIAPP aggregates-bearing exosomes decreased neuron cell survival, by the significant upregulation of cleaved caspase-3 protein levels. Then, this alteration in mitochondrial clearance observed in hippocampal cells, could also induce the accumulation of dysfunctional mitochondria and worsen or even generate the deleterious effects of Aβ or α-synuclein in Alzheimer's or Parkinson's diseases respectively. In fact, these alterations are commonly observed in those pathologies [40,41].

In summary, our results reveal the occurrence of an alternative pathway to autophagy in pancreatic β cells for eliminating aggregates of amylin through the production of exosomes, which in fact may contribute to the detoxification of those cells. The release of exosomes bearing human amylin convey the amylin aggregates to other cells such as the neuronal hippocampal cells, which in fact are severely damaged and as consequence, degenerate, suggesting an underlying molecular mechanism that may link type 2 diabetes and neurodegenerative diseases. The main results obtained in this paper are depicted in the scheme of Fig. 7.

Supplementary data to this article can be found online at https://doi.org/10.1016/j.bbamcr.2021.118971.

CRediT authorship contribution statement

Jesús Burillo: Investigation, Data curation, Visualization, Reviewing and editing. **María Fernández-Rhodes:** Investigation. **Marta Piquero M:** Methodology. **Pilar López-Alvarado:** Methodology. **José Carlos Menéndez:** Methodology. **Beatriz Jiménez:** Reviewing and editing. **Carlos González-Blanco:** Reviewing and editing. **Patricia Marqués:** Reviewing and editing. **Carlos Guillén:** Conceptualization, Supervision, Visualization, Writing, Reviewing and Editing. **Manuel Benito:** Conceptualization, Reviewing and Editing, Funding adquisition.

Declaration of competing interest

The authors declare that they have no known compe6ng financial interests or personal rela6onships that could have appeared to influence the work reported in this paper.

Acknowledgements

This work was supported by grants SAF 2017-82133-R from Ministerio de Ciencia e Innovación, MOIR2-CM B2017/BMB-3684 (Betabrain group) and Spanish Diabetes and Associated Metabolic Research Network (CIBERDEM) to M. Benito, Instituto de Salud Carlos III, Spain. We thank immunofluorescence facility core from Complutense University of Madrid for their technical assistance. We thank Gema Garcia for her technical support.

References

[1] S. Sung, J. Kim, Y. Jung, Liver-derived exosomes and their implications in liver pathobiology, Int. J. Mol. Sci. 19 (12) (2018) 3715.
[2] K. Sato, F. Meng, S. Glaser, et al., Exosomes in liver pathology, J. Hepatol. 65 (1) (2016) 213–221.
[3] C.R. Kahn, G. Wang, K.Y. Lee, Altered adipose tissue and adipocyte function in the pathogenesis of metabolic syndrome, J. Clin. Invest. 129 (10) (2019) 3990–4000.
[4] S. Kita, N. Maeda, I. Shimomura, Interorgan communication by exosomes, adipose tissue, and adiponectin in metabolic syndrome, J. Clin. Invest. 129 (10) (2019) 4041–4049.
[5] C. Guay, R. Regazzi, Exosomes as new players in metabolic organ cross-talk, Diabetes Obes. Metab. 19 (Suppl1) (2017) 137–146.
[6] Q. Ge, X.X. Xie, X. Xiao, et al., Exosome-like vesicles as new mediators and therapeutic targets for treating insulin resistance and β-cell mass failure in type 2 diabetes mellitus, J. Diabetes Res. 3256060 (2019), https://doi.org/10.1155/2019/3256060.
[7] N. Akbar, V. Azzimato, R.P. Choudhury, et al., Extracellular vesicles in metabolic disease, Diabetologia 62 (12) (2019) 2179–2187.
[8] M. Simons, G. Raposo, Exosomes—vesicular carriers for intercellular communication, Curr. Opin. Cell Biol. 21 (4) (2009) 575–581.
[9] L.H. Wong, E.R. Eden, C.E. Futter, Roles for ER: endosome membrane contact sites in ligand-stimulated intraluminal vesicle formation, Biochem. Soc. Trans. 46 (5) (2018) 1055–1062.

[10] A. Latifkar, Y.H. Hur, J.C. Sanchez, et al., New insights into extracellular vesicle biogenesis and function, J. Cell Sci. 132 (13) (2019), https://doi.org/10.1242/jcs.222406.
[11] R.A. DeFronzo, E. Ferrannini, L. Groop, et al., Type 2 Diabetes Mellitus, Nat Rev Dis Primers 1 (2015) 15019.
[12] C. Guillén, M. Benito, mTORC1 overactivation as a key aging factor in the progression to type 2 diabetes mellitus, Front. Endocrinol. (Lausanne) 9 (2018) 621.
[13] M. Garcia-Hernández, A. Garcia Aguilar, J. Burillo, et al., Pancreatic β cells overexpressing hIAPP impaired mitophagy and unbalanced mitochondrial dynamics, Cell Death Dis. 9 (5) (2018) 481.
[14] H. Farhan, M. Kundu, S. Ferro-Novick, The link between autophagy and secretion: a story of multitasking proteins, Mol. Biol. Cell 28 (9) (2017) 1161–1164.
[15] M. Zahoor, H. Farhan, Crosstalk of autophagy and the secretory pathway and its role in diseases, Int. Rev. Cell. Mol. Biol. 337 (2018) 153–184.
[16] Zhang M, Schekman R. Cell biology. Unconventional secretion, unconventional solutions. iScience, 2013;340(6132):559–561.
[17] J. Xu, R. Camfield, S.M. Gorsky, The interplay between exosomes and autophagy-partners in crime, J. Cell Sci. 131 (15) (2018).
[18] C.M. Fader, D. Sánchez, M. Furlán, et al., Induction of autophagy promotes fusion of multivesicular bodies with autophagic vacuoles in K562 cells, Traffic 9 (2) (2008) 230–250.
[19] K.M. Danzer, L.R. Kranich, W.P. Ruf, et al., Exosomal cell-to-cell transmission of alpha synuclein oligomers, Mol. Neurodegener. 7 (2012) 42.
[20] L. Alvarez-Erviti, Y. Seow, A.H. Schapira, et al., Lysosomal dysfunction increases exosome-mediated alpha-synuclein release and transmission, Neurobiol. Dis. 42 (3) (2011) 360–367.
[21] A.M. Poehler, W. Xiang, P. Spitzer, et al., Autophagy modulates SNCA/α-synuclein release, thereby generating a hostile microenvironment, Autophagy 10 (12) (2014) 2171–2192.
[22] M. Staderini, S. Aulic, M. Bartolini, et al., A fluorescent styrilquinoline with combined therapeutic and diagnostic activities against Alzheimer's and Prion diseases, ACS Med. Chem. Lett. 4 (2) (2012) 225–229.
[23] N. Bishop, A. Horman, P. Woodman, Mammalian class E Vps proteins recognize ubiquitin and act in the removal of endosomal protein-ubiquitin conjugates, J. Cell Biol. 157 (1) (2002) 91–101.
[24] L. Marzban, G. Trigo-González, C.B. Verchere, Processing of pro-islet amyloid polypeptide in the constitutive and regulated secretory pathways of β cells, Mol. Endocrinol. 19 (8) (2005) 2154–2163.
[25] M. Soty, M. Visa, S. Soriano, et al., Involvement of ATP-sensitive potassium (K (ATP)) channels in the loss of β-cell function induced by human islet amyloid polypeptide, J. Biol. Chem. 286 (47) (2011) 40857–40866.
[26] A. Ardestani, B. Lupse, Y. Kido, G. Leibowitz, K. Maedler, mTORC1 signaling: a double-edged sword in diabetic β cells, Cell Metab. 27 (2) (2018) 314–331.
[27] M. Blandino-Rosano, A.Y. Chen, J.O. Scheys, E.U. Alejandro, A.P. Gould, T. Taranukha, L. Elghazi, C. Cras-Meneur, E. Bernal-Mizrachi, mTORC1 signaling and regulation of pancreatic β-cell mass, Cell Cycle 11 (10) (2012) 1892–1902.
[28] G. Leibowitz, E. Cerasi, M. Ketzinel-Gilad, The role of mTOR in the adaptation and failure of β-cells in type 2 diabetes, Diab. Obes. Metab. 10 (Suppl. 4) (2008) 157–169.
[29] A. Bartolomé, M. Kimura-Koyanagi, S.-I. Asahara, C. Guillén, H. Inoue, K. Teruyama, S. Shimizu, A. Kanno, A. García-Aguilar, M. Koike, Y. Uchiyama, M. Benito, T. Noda, Y. Kido, Pancreatic β-cell failure mediated by mTORC1 hyperactivity and autophagic impairment, Diabetes 63 (9) (2014) 2996–3008.
[30] A. Bartolomé, C. Guillén, M. Benito, Autophagy plays a protective role in endoplasmic reticulum stress-mediated pancreatic β cell death, Autophagy 8 (12) (2012) 1757–1768.
[31] Y. Zhang, W. Song, Islet amyloid polypeptide: another key molecule in Alzheimer's pathogenesis? Prog. Neurobiol. 153 (2017) 100–120.
[32] G.J. Biessels, F. Despa, Cognitive decline and dementia in diabetes mellitus: mechanisms and clinical implications, Nat. Rev. Endocrinol. 14 (10) (2018) 591–604.
[33] X.-X. Xi, J. Sun, H.-C. Chen, A.-D. Chen, L.-P. Gao, J. Yin, Y.-H. Jing, High-fat diet increases amylin accumulation in the hippocampus and accelerates brain aging in hIAPP transgenic mice, Front. Aging Neurosci. 11 (2019) 225.
[34] H.-C. Chen, J.-X. Cao, Y.-T. Cai, Xi X.-X. du H-L, J. Sun, J. Yin, L.-P. Gao, Y.-H. Jing, Interaction of human IAPP and $A\beta_{1-42}$ aggravated the AD-related pathology and impaired the cognition in mice, Exp. Neurol. 334 (2020) 113490.
[35] J.A. Bonds, A. Shetti, T.K.L. Stephen, M.G. Bonini, R.D. Minshall, O. Lazarov, Deficits in hippocampal neurogenesis in obesity-dependent and -independent type-2 diabetes mellitus mouse models, Sci. Rep. 10 (2020) 16368.
[36] N. Fussi, M. Höllerhage, T. Chakroun, W.W. Nykänen, T.W. Rösler, T. Koeglsperger, W. Wurst, C. Behrends, G.U. Hügliger, Exosomal secretion of α-synuclein as protective mechanism after upstream blockage of macroautophagy, Cell Death Dis. 9 (7) (2018) 757.
[37] M.S. Feiler, B. Strobel, A. Freischmidt, A.M. Helferich, J. Kappel, B.M. Brewer, D. Li, D.R. Thal, P. Walther, A.C. Ludolph, K.M. Danzer, J.H. Weishaupt, TDP-43 is intercellularly transmitted across axon terminals, J. Cell Biol. 211 (4) (2015) 897–911.
[38] Y. Wang, V. Balaji, S. Kaniyappan, L. Krüger, S. Irsen, K. Tepper, R. Chandupatla, W. Metzler, A. Schneider, E. Mandelkow, E.-M. Mandelkow, The release and trans-synaptic transmission of tau via exosomes, Mol. Neurodegener. 12 (1) (2017) 5.
[39] A.S. Jadli, N. Ballasy, P. Edalat, V.B. Patel, Inside(sight) of tiny communicator: exosomes biogenesis, secretion, and uptake, Mol. Cell. Biochem. 467 (2020) 77–94.
[40] Q. Cai, P. Tammineni, Mitochondrial aspects of synaptic dysfunction in Alzheimer's disease, J. Alzheimers Dis. 57 (4) (2017) 1087–1103.
[41] A.M. Pickrell, R.J. Youle, The roles of PINK, Parkin, and mitochondrial fidelity in Parkinson's disease, Neuron 85 (2) (2015) 257–273.
[42] E. Macia, M. Ehrlich, R. Massol, E. Boucrot, C. Brunner, T. Kirchhausen, Dynasore, a cell-permeable inhibitor of dynamin, Dev Cell. 10 (6) (2006) 839–850.